

# Nonlinear optical waveguides in As<sub>2</sub>S<sub>3</sub>-Ag<sub>2</sub>S chalcogenide glass thin films

J. M. P. ALMEIDA,<sup>1,2,3</sup> E. C. BARBANO,<sup>1</sup> C. B. ARNOLD,<sup>2</sup> L. MISOGUTI<sup>1</sup>  
AND C. R. MENDONÇA<sup>1,4</sup>

<sup>1</sup>São Carlos Institute of Physics, University of São Paulo, PO Box 369, 13560-970, São Carlos, SP, Brazil

<sup>2</sup>Department of Mechanical and Aerospace Engineering, Princeton University, Princeton, NJ 08544, USA

<sup>3</sup>julianamara@ifsc.usp.br

<sup>4</sup>crmendon@ifsc.usp.br

**Abstract:** Chalcogenide glasses (ChGs) are promising materials for nonlinear optical applications due to their elevated third-order optical susceptibility. Nonetheless, oxidation and photorefractive effects make the characterization and processing of this class of materials an intricate process. Employing ultrashort laser pulses, we were able to investigate the optical nonlinearities of As<sub>2</sub>S<sub>3</sub> thin films doped with Ag<sub>2</sub>S nanocrystals, as well as produce channel waveguides. The results showed that the nonlinear refractive indexes of these films are in the order of  $2.3\text{--}5.2 \times 10^{-18} \text{ m}^2/\text{W}$  at wavelengths in the range of 775–1600 nm. Such film revealed to be proper for the development of nonlinear optical devices, since we have demonstrated the functionality of an 8.7 mm long waveguide for spectral broadening femtosecond IR pulses.

©2016 Optical Society of America

**OCIS codes:** (190.0190) Nonlinear optics; (160.2750) Glass and other amorphous materials; (310.0310) Thin films.

## References and links

1. B. J. Eggleton, B. Luther-Davies, and K. Richardson, "Chalcogenide photonics," *Nat. Photonics* **5**, 141–148 (2011).
2. A. Zakery and S. R. Elliott, "Optical properties and applications of chalcogenide glasses: a review," *J. Non-Cryst. Solids* **330**(1-3), 1–12 (2003).
3. A. B. Seddon, "Chalcogenide glasses - A review of their preparation, properties and applications.," *Non-Cryst. Solids* **184**, 44–50 (1995).
4. Y. Zou, D. N. Zhang, H. T. Lin, L. Li, L. Moreel, J. Zhou, Q. Y. Du, O. Ogbuu, S. Danto, J. D. Musgraves, K. Richardson, K. D. Dobson, R. Birkmire, and J. J. Hu, "High-Performance, High-Index-Contrast Chalcogenide Glass Photonics on Silicon and Unconventional Non-planar Substrates," *Adv. Opt. Mater.* **2**(5), 478–486 (2014).
5. Y. Zou, L. Moreel, H. Lin, J. Zhou, L. Li, S. Danto, J. D. Musgraves, E. Koontz, K. Richardson, K. D. Dobson, R. Birkmire, and J. Hu, "Solution Processing and Resist-Free Nanoimprint Fabrication of Thin Film Chalcogenide Glass Devices: Inorganic-Organic Hybrid Photonic Integration," *Adv. Opt. Mater.* **2**(8), 759–764 (2014).
6. Y. L. Zha and C. B. Arnold, "Solution-processing of thick chalcogenide-chalcogenide and metal-chalcogenide structures by spin-coating and multilayer lamination," *Opt. Mater. Express* **3**(2), 309–317 (2013).
7. Y. Zhang, G. Hong, Y. Zhang, G. Chen, F. Li, H. Dai, and Q. Wang, "Ag<sub>2</sub>S quantum dot: a bright and biocompatible fluorescent nanoprobe in the second near-infrared window," *ACS Nano* **6**(5), 3695–3702 (2012).
8. A. Tubtintae, K.-L. Wu, H.-Y. Tung, M.-W. Lee, and G. J. Wang, "Ag<sub>2</sub>S quantum dot-sensitized solar cells," *Electrochem. Commun.* **12**(9), 1158–1160 (2010).
9. K. Terabe, T. Hasegawa, T. Nakayama, and M. Aono, "Quantized conductance atomic switch," *Nature* **433**(7021), 47–50 (2005).
10. F. Nan, S. Liang, J. H. Wang, X. L. Liu, D. J. Yang, X. F. Yu, L. Zhou, Z. H. Hao, and Q. Q. Wang, "Tunable Plasmon Enhancement of Gold/Semiconductor Core/Shell Hetero-Nanorods with Site-Selectively Grown Shell," *Adv. Opt. Mater.* **2**(7), 679–686 (2014).
11. J. M. P. Almeida, C. Lu, C. R. Mendonça, and C. B. Arnold, "Single-step synthesis of silver sulfide nanocrystals in arsenic trisulfide," *Opt. Mater. Express* **5**(8), 1815–1821 (2015).
12. A. Zoubir, M. Richardson, C. Rivero, A. Schulte, C. Lopez, K. Richardson, N. Hô, and R. Vallée, "Direct femtosecond laser writing of waveguides in As<sub>2</sub>S<sub>3</sub> thin films," *Opt. Lett.* **29**(7), 748–750 (2004).
13. R. R. Gattass and E. Mazur, "Femtosecond laser micromachining in transparent materials," *Nat. Photonics* **2**(4), 219–225 (2008).

14. M. L. Miguez, E. C. Barbano, S. C. Zilio, and L. Misoguti, "Accurate measurement of nonlinear ellipse rotation using a phase-sensitive method," *Opt. Express* **22**(21), 25530–25538 (2014).
15. J. M. P. Almeida, P. H. D. Ferreira, D. Manzani, M. Napoli, S. J. L. Ribeiro, and C. R. Mendonca, "Metallic nanoparticles grown in the core of femtosecond laser micromachined waveguides," *J. Appl. Phys.* **115**(19), 193507 (2014).
16. L. Escobar-Alarcon, A. Arrieta, E. Camps, S. Muhl, S. Rodil, and E. Viguera-Santiago, "An alternative procedure for the determination of the optical band gap and thickness of amorphous carbon nitride thin films," *Appl. Surf. Sci.* **254**(1), 412–415 (2007).
17. T. Wang, X. Gai, W. H. Wei, R. P. Wang, Z. Y. Yang, X. Shen, S. Madden, and B. Luther-Davies, "Systematic z-scan measurements of the third order nonlinearity of chalcogenide glasses," *Opt. Mater. Express* **4**(5), 1011–1022 (2014).
18. D. Milam, "Review and assessment of measured values of the nonlinear refractive-index coefficient of fused silica," *Appl. Opt.* **37**(3), 546–550 (1998).
19. T. I. Kosa, R. Rangelrojo, E. Hajto, P. J. S. Ewen, A. E. Owen, A. K. Kar, and B. S. Wherrett, "Nonlinear-optical properties of silver doped As<sub>2</sub>S<sub>3</sub>," *J. Non-Cryst. Solids* **166**, 1219–1222 (1993).
20. K. A. Cerqua-Richardson, J. M. McKinley, B. Lawrence, S. Joshi, and A. Villeneuve, "Comparison of nonlinear-optical properties of sulfide glasses in bulk and thin film form," *Opt. Mater.* **10**(2), 155–159 (1998).
21. A. I. Kryukov, A. L. Stroyuk, N. N. Zin'chuk, A. V. Korzhak, and S. Y. Kuchmii, "Optical and catalytic properties of Ag<sub>2</sub>S nanoparticles," *J. Mol. Catal. A-Chemical* **221**, 209–221 (2004).
22. B. N. Chichkov, C. Momma, S. Nolte, F. vonAlvensleben, and A. Tunnermann, "Femtosecond, picosecond and nanosecond laser ablation of solids," *Appl. Phys. Adv. Mater.* **63**, 109–115 (1996).
23. X. Gai, D. Y. Choi, S. Madden, Z. Yang, R. Wang, and B. Luther-Davies, "Supercontinuum generation in the mid-infrared from a dispersion-engineered As<sub>2</sub>S<sub>3</sub> glass rib waveguide," *Opt. Lett.* **37**(18), 3870–3872 (2012).

## 1. Introduction

The large interest in nonlinear optical materials has been motivated by their potential use in all-optical devices. Chalcogenide glasses (ChGs) have received special attention due to their high refractive index and transparency over mid-infrared region. On account of the chemical nature of the elements, their nonlinear optical properties are expected to be at least one order of magnitude higher than oxide glasses [1, 2]. Arsenic trisulfide is an interesting ChG due to its photosensitive properties and flexibility to be synthesized by several routes. There are preparation methods that aim at bulk materials, such as melt-quenching, and also at thin films, in which thermal evaporation, sputtering and solution processing techniques have been employed [2, 3]. Particularly, thin film preparation has excelled because of the demand for shorter and shorter sizes, required for all-optical technologies [4, 5]. Also, many of the photoinduced effects in ChGs are more pronounced in thin films rather than bulk glasses [1]. For instance, silver photodoping of As<sub>2</sub>S<sub>3</sub> films improves the material photosensitivity [6].

Similar to arsenic trisulfide, silver sulfide (Ag<sub>2</sub>S) is also a promising semiconductor for infrared technologies. When synthesized as nanocrystals or quantum dots it can be used as NIR emitters, sensitizers for solar cells and atomic switches [7–9]. Moreover, Ag<sub>2</sub>S nanocrystals present tunable emission in the near infrared and photocatalytic properties [10], which combined with the ChG can result in an advanced material for photonics. Recently, we demonstrated a simple method to fabricate thin films of glassy As<sub>2</sub>S<sub>3</sub> doped with Ag<sub>2</sub>S nanocrystals [11]. Nonetheless, for improving infrared technologies, it is essential to develop and characterize new materials as well as determine optimal processing for practical applications in all-optical systems.

Among the techniques for materials processing, direct laser writing (DLW) has been remarkable due to the variety of processes that can be controlled. Printing, sintering, ablation and optical properties manipulation of different classes of materials can be accomplished when using DLW [12]. These processes can reach the micro/nanoscale and adverse thermal effects can be avoided if fs-laser pulses are employed [13].

Besides the importance of fs-laser for short-scale materials processing, it is also crucial for characterization of optical nonlinearities. The characterization of nonlinear optical properties of thin films is particularly difficult because the magnitude of the investigated signal depends on the thickness. Thus, to check the material response, the beam intensity has to be increased, which on the other hand may damage the irradiated region.

Although nonlinear optical properties and photonic devices have been demonstrated mostly in bulk ChG, studies on ultrashort pulse regime for processing and characterization of ChGs thin film are yet limited. In the present paper fs-pulses are used to study third-order optical nonlinearities and fabricate optical waveguides in ChGs containing semiconductor nanocrystals. Specifically, 500-nm films of  $\text{As}_2\text{S}_3$  and  $\text{As}_2\text{S}_3$  doped with  $\text{Ag}_2\text{S}$  nanocrystals ( $\text{As}_2\text{S}_3:\text{Ag}_2\text{S}\text{-NCs}$ ) were produced from spin-coating the precursor solutions on glass substrates [11]. Because those films present low damage threshold, the nonlinear index of refraction was evaluated in the range of 775 – 1600 nm using nonlinear ellipse rotation (NER) approach [14], which is a phase-sensitive method suitable for measuring such kind of sample. The Kerr effect of ChGs investigated herein is high enough to allow the application of the waveguides produced by fs-DLW in spectral broadening devices.

## 2. Materials and methods

The synthesis of  $\text{As}_2\text{S}_3$  and  $\text{As}_2\text{S}_3:\text{Ag}_2\text{S}\text{-NCs}$  thin films was described in ref [11]. Briefly, arsenic trisulfide solution is prepared with a concentration of 133g/L by the dissociation of the precursor ( $\text{As}_2\text{S}_3$  alfa aesar 99.999%) in n-propylamine ( $\text{C}_3\text{H}_9\text{N}$  Sigma-Aldric >99%) at room temperature. The *in situ* synthesis of  $\text{Ag}_2\text{S}$  nanocrystals is achieved by mixing 1 ml of the previous solution with 0.25 ml of  $\text{AgCl}$  [80g/L] also in n-propylamine. Both  $\text{As}_2\text{S}_3$  and  $\text{As}_2\text{S}_3:\text{Ag}_2\text{S}\text{-NCs}$  solutions were spin-coated in glass coverslips, 150- $\mu\text{m}$  thick, and then annealed at 60 °C/1h + 110 °C/7h for solvent removal. The whole process was carried out in inert atmosphere to avoid water contamination.

The spectrum of nonlinear refractive index ( $n_2$ ) was determined by NER technique, which is a phase-sensitive method and measured with a dual-phase lock-in amplifier [14]. In the NER technique a zero-order quarter-waveplate was used to change the laser beam polarization from linear to elliptical. The elliptical polarized light was focused (3 cm focal length) into the sample which was translated through the focal position. A spinning analyzer was placed after the sample and then the beam was focused on a photodetector. Monitoring the signal with a dual-phase lock-in amplifier, it is possible to determine the nonlinear ellipse rotation, which enables one to obtain the  $n_2$  [14]. An optical parametric amplifier (OPA) was employed as excitation light source and provides pulses of 120 fs, in the spectral range of 460 to 2600 nm. The OPA is pumped by a Ti:Sapphire amplified system (CPA 2001, Clark MXR) at 775 nm with 150 fs pulse duration at 1 kHz repetition rate. The pulse energies (irradiances) and beam waist radius ranged from 15 to 110 nJ (or 46 to 362  $\text{GW}/\text{cm}^2$ ) and 6.3 to 7.5  $\mu\text{m}$ , respectively, depending on the excitation wavelength. Because the thin films were produced on glass coverslips, the resulting nonlinear signal corresponds to both film and substrate contributions. Thus, in order to discriminate them, the substrate itself was evaluated separately. The magnitude of NER signal is proportional to the film thickness, which was measured by atomic force microscopy (AFM) from a mechanically removed line on the sample center. Sample thicknesses were  $530 \pm 20$  nm and  $552 \pm 7$  nm for  $\text{As}_2\text{S}_3$  and  $\text{As}_2\text{S}_3:\text{Ag}_2\text{S}\text{-NCs}$ , respectively.

Direct laser writing experiments were performed with a Ti:Sapphire oscillator laser at 800 nm, operating at 5 MHz with pulses of 50 fs. The sample was moved by motorized stages at 10  $\mu\text{m}/\text{s}$  perpendicularly to the laser beam, which was focused on film surface with a  $40\times$  ( $\text{NA} = 0.65$ ) objective. After determining the damage threshold energy, curved waveguides were fabricated through subtractive microfabrication, in which a pre-determined pattern is produced by material removal. To evaluate the waveguide loss and its use in spectral broadening, we used a set-up composed by microscopes objectives (details in ref [15].) to coupling/collect the light from a He-Ne (632.8 nm) or fs-laser (Clark MXR) in the waveguides.

### 3. Results and discussion

Figure 1 shows the transmittance spectra of  $\text{As}_2\text{S}_3$  and  $\text{As}_2\text{S}_3:\text{Ag}_2\text{S}$ -NCs samples, in which interference fringes are due to the thin thickness. The absorption edges, determined by Absorbance Spectrum Fitting method [16] are 541 nm (2.29 eV) and 537 nm (2.31 eV) for undoped and doped films, respectively. For nonlinear refractive index determination, NER measurements were performed at the infrared region, where the samples are transparent. The values of  $n_2$  in function of the wavelength are shown in Fig. 2, which also displays the NER signature at 775 nm for samples and substrate (inset). Differences between the phase magnitude of the substrate and ChG samples indicate the optical nonlinearity of the thin films themselves. Low dispersion is observed in the investigated region (775-1600 nm), which correspond to average  $n_2$  values of  $5.2 \times 10^{-18} \text{ m}^2/\text{W}$  and  $2.3 \times 10^{-18} \text{ m}^2/\text{W}$  for  $\text{As}_2\text{S}_3$  and  $\text{As}_2\text{S}_3:\text{Ag}_2\text{S}$ -NCs films, respectively.

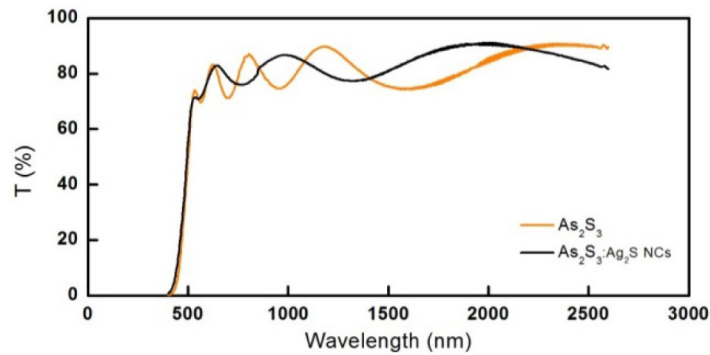


Fig. 1. Transmittance spectra of undoped ( $\text{As}_2\text{S}_3$ ) and  $\text{Ag}_2\text{S}$ -NCs doped thin films.

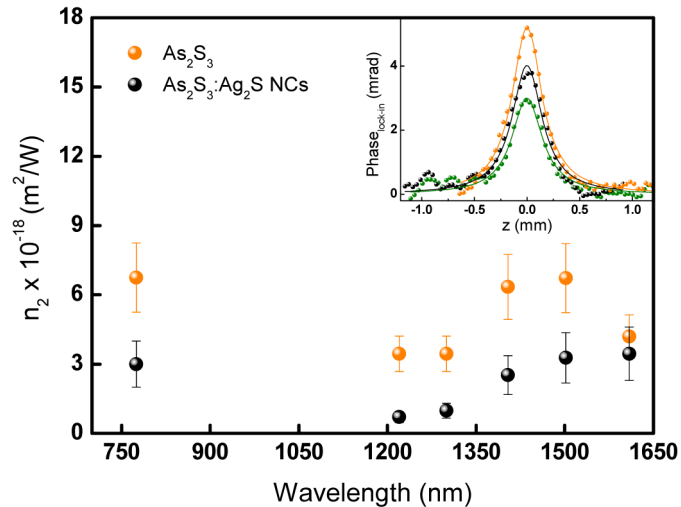


Fig. 2. Spectra of the nonlinear refractive index of  $\text{As}_2\text{S}_3$  and  $\text{As}_2\text{S}_3:\text{Ag}_2\text{S}$ -NCs thin films obtained by nonlinear ellipse rotation (NER). The inset displays the NER curves at 775 nm for both samples on the substrate and the substrate itself (green curve) for comparison.

The  $n_2$  value obtained herein for pure  $\text{As}_2\text{S}_3$  is slightly higher than the one reported for the bulk sample ( $2.9 \times 10^{-18} \text{ m}^2/\text{W}$  [17]), while it is almost 20 times the value of fused silica ( $2.8 \times 10^{-19} \text{ m}^2/\text{W}$  [18]), both at 1550 nm. It is worth mentioning, however, that the absolute value of the nonlinear refractive index of a- $\text{As}_2\text{S}_3$  is a matter of debate [17, 19, 20]. Moreover, a few works have been dedicated to thin film characterization, particularly at femtosecond regime.

For instance, in Ref [20], self-phase modulation was used to estimate the  $n_2$  of  $\text{As}_{40}\text{S}_{60}$  film as  $8 \pm 4 \times 10^{-19} \text{ m}^2/\text{W}$  (at  $1.5 \mu\text{m}$  and  $500 \text{ fs}$ ).

As seen in Fig. 2, the addition of semiconductor NCs caused a reduction of the  $n_2$ , which is in accordance with the increasing of the bandgap energy of the doped film. Despite such reduction,  $\text{Ag}_2\text{S}$  NCs doping is valuable because it aggregates quantum confinement effects to the material, including tunable emission in the NIR [21]. Thus, taking advantage of the high nonlinear refractive index of ChGs, we investigated the ability to produce a nonlinear waveguide using DLW with fs-laser pulses. To determine the damage threshold energy ( $E_{th}$ ), a set of grooves were produced by changing the pulse energy ( $E$ ), as shown in Fig. 3. The variation of groove widths ( $L$ ) corresponds to a logarithmic behavior described by  $L \approx \alpha^{-1} \ln(E/E_{th})$ , where  $\alpha^{-1}$  is the optical penetration depth [22]. Through the fitting of the experimental data, one obtains  $E_{th}$  of  $0.50 \pm 0.06$  and  $0.39 \pm 0.06 \text{ nJ}$  ( $600$  and  $470 \text{ GW}/\text{cm}^2$ ) for pure and doped ChGs respectively, representing the lower energies to cause material removal. Varying the pulse energy used for DLW it is possible to control the groove width in the range of approximately  $1 - 5 \mu\text{m}$ . As an example, the inset of Fig. 3 displays an AFM image of a sharp groove produced with  $E = 1.5 \text{ nJ}$  on  $\text{As}_2\text{S}_3:\text{Ag}_2\text{S}$ -NCs, being close to the threshold energy.

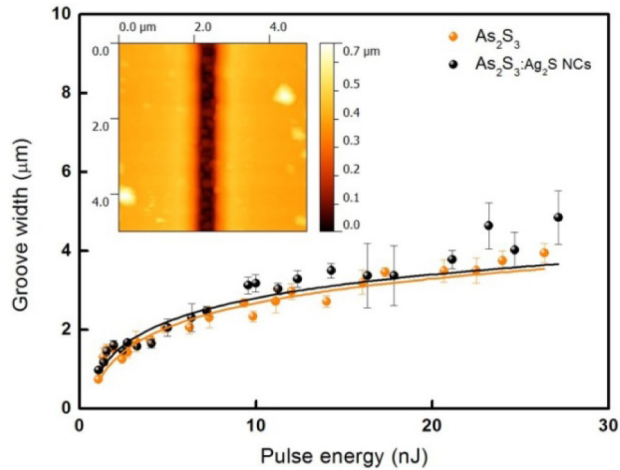


Fig. 3. Groove width on the surface of  $\text{As}_2\text{S}_3$  and  $\text{As}_2\text{S}_3:\text{Ag}_2\text{S}$ -NCs thin films as a function of the pulse energy, for scan speed of  $10 \mu\text{s}$ , using an objective lens of  $\text{NA} = 0.65$ . The solid lines represent the fit obtained with the equation given in the text. The inset shows an AFM image of a groove fabricated on doped film with pulse energy close to  $E_{th}$ .

The DLW of two parallel grooves throughout the film provide a high contrast refractive index represented by the interfaces of air/ChGs/air, which enabled the design of a waveguide. Figure 4 shows the functionality of a curved waveguide, fabricated on the doped ChG with a length of  $8.7 \text{ mm}$  and cross-section of  $36 \times 0.5 \mu\text{m}$ , in the configuration of a channel waveguide. The image in Fig. 4 shows the top view of the waveguide, wherein a red light from a HeNe laser was coupled using a microscope objective. One can note the light confinement at the borders of the waveguide corresponding to the propagation modes. Propagation loss of  $5.8 \pm 0.6 \text{ dB}/\text{cm}$  at  $632.8 \text{ nm}$  was quantified by the intensity reduction throughout waveguide, using image processing software. The main loss mechanism is attributed to the scattering from roughness induced by the DLW process and/or to the wavelength proximity to the material absorption edge. Thus, such loss could be severely reduced at NIR, which is the most interesting region for ChG application. For instance, single mode  $\text{As}_2\text{S}_3$  waveguides produced by photolithography can achieve values  $> 6 \text{ dB}/\text{cm}$  at telecom region and  $0.75 \pm 0.05 \text{ dB}/\text{cm}$  at  $3.6 \mu\text{m}$  [20, 23].

Thus, although the coupling of visible light facilitates the waveguide characterization and observation of guided modes, it is not the proper working region due to the proximity to the material absorption edge and the predominance of photorefractive effect. Nonetheless, even at 632.8 nm, it is possible to observe light reaching the end of the curved waveguide after the propagation along 8.7 mm, enabling its application in all-optical circuits in a wide wavelength range. The advantage of fs-DLW over other methods relies on its capability of producing waveguide with high scan speeds in a single processing step.

In order to demonstrate its usage as a nonlinear waveguide, fs-laser pulses (775 nm) were coupled into the waveguide of Fig. 4 and revealed a spectral broadening from 750 to 800 nm, as illustrated in the inset. For such spectral broadening we use an average power of 55 mW at the waveguide entrance. It is known that the increase of such pump power leads to a wider supercontinuum generation, but care must be taken to avoid reaching the sample damage threshold. From the values of the nonlinear refractive index (Fig. 2), one can determine the nonlinear coefficient of the waveguide, represented by  $\gamma = 2\pi n_2 / (\lambda A_{eff})$ , where  $A_{eff}$  is the simulated effective mode area. At 775 nm  $\gamma$  is on the order of  $1 \text{ W}^{-1} \text{ m}^{-1}$ , which is twice larger than the one reported for  $\text{As}_2\text{S}_3$  rib waveguide pumped at 3260 nm [23]. Therefore, the results reported herein demonstrate the applicability of chalcogenide thin films for the development of nonlinear waveguides. Moreover, the fs-laser based techniques employed for material characterization and processing are also effective for determining the optical nonlinearities and fabricating curved channel waveguides. Such methods allow the exploration of several classes of thin films, including doped ones, which could encompass new features to the material system, as the quantum confinement effect associated with NCs.

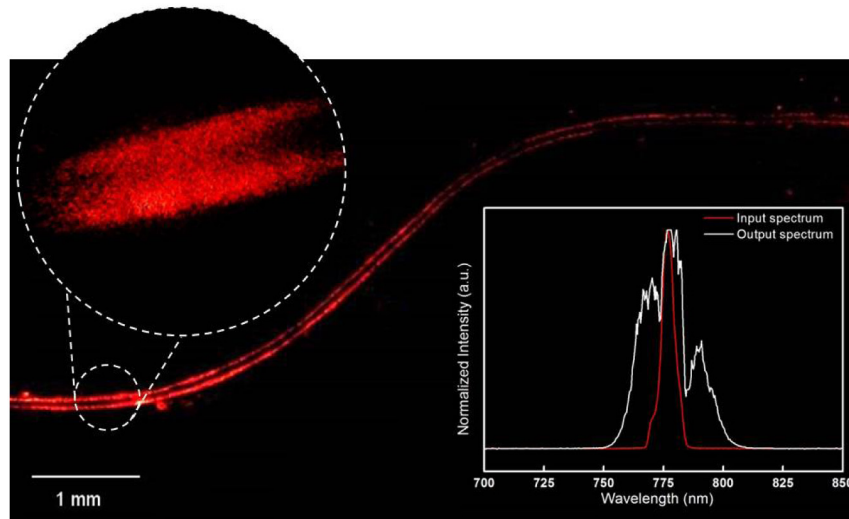


Fig. 4. Curved 8.7 mm-long waveguide fabricated on the doped sample through the removal of fs-laser irradiated regions. The inset shows the spectral broadening (output) of a fs-laser at 775 nm (input).

#### 4. Conclusion

We employed nonlinear ellipse rotation (NER) and direct laser writing (DLW) with ultrashort pulses to characterize optical nonlinearities and fabricate photonic devices in thin films of chalcogenide glasses (ChGs). The nonlinear refractive index of 500-nm thick  $\text{As}_2\text{S}_3$  films does not show significant dispersion in the range of 775 – 1600 nm, being approximately  $5.2 \times 10^{-18} \text{ m}^2/\text{W}$ , which is slightly higher (~2 fold) than the one reported for the bulk sample. The doping with  $\text{Ag}_2\text{S}$  nanocrystals (NCs) caused a reduction on  $n_2$  to  $2.3 \times 10^{-18} \text{ m}^2/\text{W}$ ,

although it is interesting for combining the properties of semiconductor NCs to the ChG. Using fs-DLW, we find the damage threshold energy ( $E_{th}$ ) of  $As_2S_3$  and  $As_2S_3:Ag_2S$ -NCs films to be  $0.50 \pm 0.06$  and  $0.39 \pm 0.06$  nJ, respectively. Applying pulse energy close to  $E_{th}$ , grooves of  $\sim 1$   $\mu m$  can be produced. The material processing with fs-DLW enabled the fabrication of an 8.7-mm long curved waveguide, with propagation loss of  $5.8 \pm 0.6$  dB/cm at 632.8 nm on the doped film. Such waveguides can be used as a nonlinear optical device for the infrared.

### Funding

We acknowledge FAPESP (2013/05350-0, 2011/12399-0 and 2015/17058-7) for the financing and for supporting JMP Almeida's internship at Princeton University, as well as the PU-USP partnership program. We also thank NSF (EEC-0540832 and DMR-1420541), CNPq and CAPES for the financial support.